

Evolution of a cool phonon pulse propagating in superfluid helium

I. N. Adamenko,¹ K. E. Nemchenko,¹ V. A. Slipko,¹ and A. F. G. Wyatt²

¹Karazin Kharkov National University, Svobody Sq. 4, Kharkov, 61077, Ukraine

²School of Physics, University of Exeter, Exeter EX4 4QL, United Kingdom

(Received 31 March 2003; published 6 October 2003)

We derive the system of equations which describes the evolution of a cool phonon pulse during its propagation in superfluid helium. Solutions are found both for longitudinal deformation of the pulse along the pulse axis and for the transverse evolution perpendicular to the pulse axis. It is shown that the longitudinal motion of the pulse is described by a simple running wave, and the transverse evolution is similar to the expansion of a gas in a vacuum. From these solutions, the angular distribution of phonon-energy density is calculated at various distances from the source. We discuss the very unusual evolution of the phonon pulse and compare it to experimentally observed phenomena.

DOI: 10.1103/PhysRevB.68.134507

PACS number(s): 67.40.Fd

I. INTRODUCTION

Phonon pulses created by a heater in superfluid helium are strongly anisotropic and nonuniform systems.¹⁻³ They possess many unique properties, one of which is the creation of high-energy phonons (*h*-phonons) by a propagating pulse of low-energy phonons (*l*-phonons) in liquid helium.¹⁻³ This phenomenon is explained by theory,^{4,5} and new ones are predicted.⁶⁻⁸ However, a number of experimental observations remain unexplained. It is found that *h*-phonons are created at large distances from the source.³ The distances are much greater than those calculated assuming geometrical expansion of the transverse dimensions of the pulse,⁹ which causes rapid cooling of the *l*-phonons which essentially stops the creation of *h*-phonons within a short distance from the heater.

The measured angular dependence of the detected signal,^{2,10} its development with distance, and its dependence on input power and pulse length show that its evolution is complex, and is not consistent with the model of geometric expansion.

To understand the experimental data it is necessary to develop a theory of the evolution of a phonon pulse during its propagation from a heater to a detector. In this paper we assume that there is instantaneous three-phonon relaxation. We then obtain equations for the *l*-phonon energy density and find a number of solutions that describe the evolution of a relatively cool pulse of *l*-phonons during its motion in superfluid helium.

II. THE EQUATIONS THAT DESCRIBE THE EVOLUTION OF A PHONON PULSE

A pulse of phonons in superfluid helium, as any other quasiparticle system, can be described completely by the quasiclassical distribution function $n(\mathbf{p}, \mathbf{r}, t)$ which determines the number of phonons at time t in phase volume element $(2\pi\hbar)^3$ which includes the point of six-dimensional phase space \mathbf{p}, \mathbf{r} . The temporal evolution of the phonon pulse is described by the kinetic equation,

$$\frac{\partial n}{\partial t} + \frac{\partial n}{\partial \mathbf{r}} \frac{\partial \varepsilon}{\partial \mathbf{p}} = I_{3PP} + I_{4PP}. \quad (1)$$

Here I_{3PP}, I_{4PP} are collision integrals which change the number of phonons in the quantum state in unit time due to three-phonon and four-phonon processes, respectively. The phonon energy ε can be written as

$$\varepsilon = cp[1 + \Psi(p)], \quad (2)$$

where p is the phonon momentum and the function $\Psi(p)$ describes the deviation of the phonon energy-momentum relation from a linear dependence. In superfluid helium this deviation is small [$\Psi(p) \ll 1$], nonetheless it determines the various mechanisms of phonon relaxation.^{11,12}

At the saturation vapor pressure, the function $\Psi(p < p_c = \varepsilon_c/c)$ is positive (anomalous dispersion) for phonons with $\varepsilon < \varepsilon_c = 10$ K.¹¹⁻¹³ With this dispersion, three-phonon processes are allowed and the collision integral I_{3PP} is nonzero. At $\varepsilon > \varepsilon_c$, the function $\Psi(p)$ is negative (normal dispersion). In this case three-phonon processes are not allowed as energy and momentum cannot be conserved.^{14,15} So for high energy phonons with ($\varepsilon > \varepsilon_c$) the most rapid processes are four-phonon processes,¹⁶ which in Eq. (1) are described by the collision integral I_{4PP} .

The lifetime due to three-phonon processes τ_{3PP} is calculated with the Landau Hamiltonian in first-order perturbation theory,^{17,18} and the lifetime due to four-phonon processes τ_{4PP} is calculated in second-order perturbation theory.¹⁹ This is the reason for the strong inequality

$$\tau_{3PP} \ll \tau_{4PP}, \quad (3)$$

which is confirmed by numerous experiments.

According to inequality (3), phonons in superfluid helium form two subsystems with substantially different relaxation times. The first subsystem is low-energy phonons (*l*-phonons) with $\varepsilon < \varepsilon_c$, in which equilibrium is attained instantaneously on the scale of all other relevant times. The second subsystem is high-energy phonons (*h*-phonons) with $\varepsilon > \varepsilon_c$, in which equilibrium is attained relatively slowly.

Using the result of Ref. 20 the initial distribution n_0 of phonons that form the pulse can be written as

$$n_0 = n(\mathbf{p}, \mathbf{r}, t=0) = \frac{\eta(\mathbf{p}\mathbf{e}_z/p - \cos \theta_{3PP})}{\exp[\varepsilon/T_0(\mathbf{r})] - 1}, \quad (4)$$

where η is the step function, which is equal to unity or zero for positive or negative values of the argument respectively, and \mathbf{e}_z is the unit vector, directed along the z axis. The initial distribution (4) describes a pulse of phonons, localized in space, where the temperature $T_0(\mathbf{r})$ is greater than zero. According to Eq. (4), such a pulse is an anisotropic phonon system in which the momenta of all phonons lie within a narrow cone of angle θ_{3PP} which is of order of the typical angle for three-phonon processes. At $t=0$, the axis of the cone is directed along the z axis at every point inside the pulse. The strongly anisotropic and nonuniform system of phonons studied here was observed in experiments^{1-3,10} in superfluid helium at such a low temperature that the thermal excitations of helium can be neglected. Such superfluid helium can be considered to be a “superfluid vacuum” in which the phonons propagate. At time $t=0$ the heater creates a phonon pulse with the initial distribution (4). The size of the pulse along the x and y axes is determined by the size of the heater and the pulse duration t_p .

The evolution of a phonon pulse as a function of time during its motion in the superfluid vacuum can be described by the equations that express the conservation of energy and momentum. These equations are obtained by multiplying Eq. (1) by energy or momentum and then integrating with respect to momentum:

$$\frac{\partial E(\mathbf{r}, t)}{\partial t} + \frac{\partial \mathbf{Q}_E(\mathbf{r}, t)}{\partial \mathbf{r}} = 0, \quad (5)$$

$$\frac{\partial P_i(\mathbf{r}, t)}{\partial t} + \frac{\partial Q_{ij}(\mathbf{r}, t)}{\partial r_j} = 0, \quad (6)$$

where

$$E(\mathbf{r}, t) = \int \varepsilon n \frac{d^3 p}{(2\pi\hbar)^3} \quad (7)$$

is the phonon density energy,

$$\mathbf{Q}_E(\mathbf{r}, t) = \int \varepsilon \frac{\partial \varepsilon}{\partial \mathbf{p}} n \frac{d^3 p}{(2\pi\hbar)^3} \quad (8)$$

is vector of the energy density flux,

$$\mathbf{P}(\mathbf{r}, t) = \int \mathbf{p} n \frac{d^3 p}{(2\pi\hbar)^3} \quad (9)$$

is the phonon momentum density,

$$Q_{ij}(\mathbf{r}, t) = \int p_i \frac{\partial \varepsilon}{\partial p_j} n \frac{d^3 p}{(2\pi\hbar)^3} \quad (10)$$

is the tensor of phonon-momentum density flux.

III. THE CHOICE OF THE SOLUTION OF THE KINETIC EQUATION

The distribution function n appearing in Eqs. (7)–(10) is a solution of the integro-differential equation (1) with initial condition (4). Taking into account that the three-phonon relaxation is fast, the required solution can be written as follows:

$$n(\mathbf{p}, \mathbf{r}, t) = n_\Omega(\mathbf{p}, \mathbf{r}, t) + n_I(\mathbf{p}, \mathbf{r}, t), \quad (11)$$

where $n_\Omega(\mathbf{p}, \mathbf{r}, t)$ is the local equilibrium distribution function, which makes the collision integrals I_{3PP} , I_{4PP} equal to zero, and $n_I(\mathbf{p}, \mathbf{r}, t)$ is the additional term which is small for small values of the times τ_{3PP} and τ_{4PP} .

If we do not consider the dissipative relaxation in the phonon pulse, we retain only the first term in Eq. (11). This is a good approximation for three-phonon processes which describe the most important phenomena taking place in the pulse. The four-phonon processes result in an intensive creation of h -phonons and a loss of energy from the l -phonon subsystem, in highly-anisotropic phonon systems.⁵ If we omit the second term in Eq. (11), this process will not be considered.

In this paper we retain only the first term in Eq. (11). In this approximation only the evolution of l -phonon pulse will be described and the contribution of h -phonons to all processes will be ignored. Obviously, this approximation is only correct for sufficiently cool pulses. For hot pulses, this approximation is only valid from the time when the l -phonon pulse has become so cold that the creation of h -phonons can be neglected.

We now discuss the choice of the local equilibrium function. As is known, such a function is the Bose-Einstein distribution function with parameters that depend on time and spatial coordinates. Here one must take into account the strong anisotropy of the phonon pulse and the fast three-phonon processes. These instantaneously (on the scale of all typical times in the problem) provide equilibrium in a cone with small angle θ_{3PP} , which is typical for the three-phonon processes. When the isotropic phonon system was considered in Ref. 21 it was supposed that the parameters of the Bose-Einstein distribution function depended on direction. Such an approximation needs $\theta_{3PP} = 0$.

For a strongly anisotropic phonon system this approximation is not acceptable, since the finite value of angle θ_{3PP} explains several phenomena^{2,10,22} that take place in phonon pulses.

For one variant of the solution of our problem, consider the Bose-Einstein local equilibrium function that includes the hydrodynamic velocity $\mathbf{u}(\mathbf{r}, t)$:

$$n_\Omega(\mathbf{p}, \mathbf{r}, t) = \frac{\eta(\mathbf{p}\mathbf{e}_z/p - \cos \theta_{3PP})}{\exp[(\varepsilon - \mathbf{p}\mathbf{u})/T] - 1}. \quad (12)$$

Substituting Eq. (12) into relations (5)–(10) gives the system of four equations for the four desired functions $\mathbf{u}(\mathbf{r}, t)$ and $T(\mathbf{r}, t)$, which, according to Eq. (4), satisfy the initial conditions

$$\mathbf{u}(\mathbf{r}, t=0) = 0; \quad T(\mathbf{r}, t=0) = T_0(\mathbf{r}). \quad (13)$$

From the solution of this system of four equations, with initial conditions (13), it follows that after a time of order of the length of the heat pulse t_p (which creates the phonon pulse with size $L = t_p c$ moving along the axis z) the z component of the hydrodynamic velocity becomes so close to c that function (12) becomes strongly anisotropic inside the cone with angle θ_{3PP} . This anisotropy results from the fact that after a time t_p almost all phonons will move along the axis z , and the number of phonons moving at the angle θ_{3PP} to the z axis will be small. This solution contradicts the collision integral I_{3PP} , since it describes three-phonon processes, which practically instantaneously (in time $\tau_{3PP} \ll t_p$) destroy this anisotropy within a cone of angle θ_{3PP} .

The solution that does not have this inconsistency can be written in the form

$$n_{\Omega}(\mathbf{p}, \mathbf{r}, t) = \frac{\eta(\mathbf{ps}/p - \cos \theta_{3PP})}{\exp(\varepsilon/T) - 1}, \quad (14)$$

where the unit vector $\mathbf{s}(\mathbf{r}, t)$ determines the direction of the axis of the cone with angle θ_{3PP} , at any moment of time t and at any spatial point \mathbf{r} inside the pulse.

Substituting Eq. (14) into relation (5)–(10) gives a system of four equations for three functions since

$$\mathbf{s}^2 = 1. \quad (15)$$

As will be shown below, this system of four equations is not independent and gives a system of three independent equations for the three required functions of temperature $T(\mathbf{r}, t)$ and any two functions that determine the direction of vector $\mathbf{s}(\mathbf{r}, t)$. These, according to Eq. (4), should satisfy the initial condition:

$$\mathbf{s}(\mathbf{r}, t=0) = \mathbf{e}_z \quad \text{and} \quad T(\mathbf{r}, t=0) = T_0(\mathbf{r}). \quad (16)$$

Solution (14) determines the nonuniform and anisotropic phonon system, in which the instantaneous equilibrium takes place in the cone directed along the vector \mathbf{s} and with angle θ_{3PP} which is equal to the typical angle for three-phonon processes.

It should be noted that the angle θ_{3PP} depends on the typical momenta of phonons taking place in three-phonon processes. This causes θ_{3PP} to be a function of temperature. Moreover, according to estimates made first in Ref. 23 the frequent three-phonon collisions result in the diffusion of phonons in angular space. Later this problem for the case of small deviation from equilibrium was studied in detail in Ref. 24. Such a diffusion results in an explicit dependence of θ_{3PP} on time. In order to obtain the full dependences on temperature and time, one should solve a sufficiently complete nonlinear mathematical problem. To avoid this we here restrict ourselves to a solution with a constant value of θ_{3PP} .

IV. EVOLUTION EQUATIONS FOR THE PARAMETERS OF THE LOCAL EQUILIBRIUM DISTRIBUTION FUNCTION

Using the dispersion law (2) for the energy density of l -phonons (7) in the linear approximation with respect to the

small parameter Ψ , we obtain

$$E(\mathbf{r}, t) = \frac{3!2\pi\zeta(4)k_B^4}{(2\pi\hbar c)^3} \zeta_p(T^4 + \chi - T\chi'), \quad (17)$$

where $\zeta(m)$ is Riemann zeta function,

$$\zeta_p = 1 - \cos \theta_{3PP}, \quad (18)$$

$$\chi = \chi(T) = \frac{1}{3!\zeta(4)} \int_0^\infty \Psi(\varepsilon) \frac{\varepsilon^3 d\varepsilon}{\exp(\varepsilon/T) - 1}, \quad (19)$$

and the primed function denotes the derivative with respect to the argument.

Let us estimate the numerical value of the nondimensional function χ/T^4 , which is included to Eq. (17). According to Ref. 5, a good approximation for the deviation of the phonon energy-momentum relation from a linear dependence can be written as follows:

$$\Psi(\varepsilon) = \gamma_d \left(\frac{\varepsilon}{\varepsilon_c} \right)^2 \left[1 - \left(\frac{\varepsilon}{\varepsilon_c} \right)^2 \right], \quad (20)$$

where

$$\gamma_d = \frac{c - \partial\varepsilon/\partial p|_{\varepsilon=\varepsilon_c}}{2c}. \quad (21)$$

Using the experimental values $c = 238 \text{ ms}^{-1}$, $\partial\varepsilon/\partial p|_{\varepsilon=\varepsilon_c} = 189 \text{ ms}^{-1}$ we have $\gamma_d = 0.103$. Substituting Eq. (20) into Eq. (19) gives

$$\frac{\chi(T)}{T^4} = \frac{\gamma_d}{3!\zeta(4)} \left(5!\zeta(6) \frac{T^2}{\varepsilon_c^2} - 7!\zeta(8) \frac{T^4}{\varepsilon_c^4} \right). \quad (22)$$

Using the numerical values of γ_d and known values of Riemann zeta functions [$\zeta(4) = 1.082$, $\zeta(6) = 1.017$, and $\zeta(8) = 1.004$] we get at typical temperature $T = 1 \text{ K}^{1-3,10}$

$$\frac{\chi(T)}{T^4} \Big|_{T=1 \text{ K}} = 0.011. \quad (23)$$

Value (23) is close to the numerical value of ζ_p , which, according to Refs. 2 and 20, is equal to 0.02. This result is natural because the value of ζ_p , as well as function (23), is determined by the small deviation of the phonon energy-momentum relation from linearity. So in the following calculations, we will consider only linear terms with respect to these two small parameters χ/T^4 and ζ_p , which have equal orders of magnitude.

Relations (2), (8)–(10) in this approximation give

$$\mathbf{Q}_E(\mathbf{r}, t) = \frac{3!\zeta(4)k_B^4\zeta_p}{(2\pi c)^2\hbar^3} \left[\left(1 - \frac{\zeta_p}{2} \right) T^4 - 2\chi \right] \mathbf{s}; \quad (24)$$

$$\mathbf{P}(\mathbf{r}, t) = \frac{3!\zeta(4)k_B^4\zeta_p}{(2\pi)^2\hbar^3 c^4} \left[\left(1 - \frac{\zeta_p}{2} \right) T^4 - T\chi' \right] \mathbf{s}; \quad (25)$$

$$Q_{ij}(\mathbf{r}, t) = \frac{3! \zeta(4) k_B^4 \zeta_p}{(2\pi)^2 (\hbar c)^3} \left[\frac{\zeta_p}{2} T^4 \delta_{ij} + \left(\left\{ 1 - \frac{3\zeta_p}{2} \right\} T^4 - 3\chi \right) s_i s_j \right]. \quad (26)$$

Substituting relations (17), (24)–(26) into Eqs. (5) and (6) we get in the linear approximation with respect to small parameters ζ_p and χ/T^4 the following system of three independent equations:

$$\frac{\partial T^4}{c \partial t} + \left[1 - \frac{\zeta_p}{2} + \frac{T\chi'' - 2\chi'}{4T^3} \right] \frac{\partial T^4}{\partial z} + \frac{\partial}{\partial x} (T^4 s_x) + \frac{\partial}{\partial y} (T^4 s_y) - \frac{1}{2} \frac{\partial}{\partial z} [T^4 (s_x^2 + s_y^2)] = 0; \quad (27)$$

$$\frac{\partial}{c \partial t} (T^4 s_x) + \frac{\partial}{\partial z} (T^4 s_x) + \frac{\partial}{\partial x} \left[T^4 \left(\frac{\zeta_p}{2} + s_x^2 \right) \right] + \frac{\partial}{\partial y} (T^4 s_x s_y) = 0; \quad (28)$$

$$\frac{\partial}{c \partial t} (T^4 s_y) + \frac{\partial}{\partial z} (T^4 s_y) + \frac{\partial}{\partial y} \left[T^4 \left(\frac{\zeta_p}{2} + s_y^2 \right) \right] + \frac{\partial}{\partial x} (T^4 s_x s_y) = 0; \quad (29)$$

where we introduce the general notation $r_1 = x$, $r_2 = y$, $r_3 = z$, $s_1 = s_x$, $s_2 = s_y$, and $s_3 = s_z$.

This system of three equations for the three desired functions $T(\mathbf{r}, t)$, $s_x(\mathbf{r}, t)$, and $s_y(\mathbf{r}, t)$ is completed by the initial conditions

$$s_x(\mathbf{r}, t=0) = 0; \quad s_y(\mathbf{r}, t=0) = 0; \quad T(\mathbf{r}, t=0) = T_0(\mathbf{r}). \quad (30)$$

During the derivation of Eqs. (27)–(29) we take into account that, from the initial conditions (30) for s_x and s_y and the system of Eqs. (5) and (6), the values s_x and s_y are small and are of order $\sqrt{\zeta_p}$. In the calculations presented below we find that $s_x, s_y \sim \sqrt{\zeta_p/2} = 0.1$.

It is easy to check that Eq. (6), for $i=3$ rewritten in the same approximation as Eqs. (27)–(29), coincides with Eq. (27), which expresses the conservation of energy. As a result the system of four equations becomes a system of three independent equations.

V. EVOLUTION OF THE PHONON PULSE IN THE DIRECTION OF ITS MOTION

The phonon pulse, propagating in superfluid vacuum He II, cannot be described even approximately in a model where the deviation from equilibrium is weak. So, one should solve the nonlinear system of three differential Eqs. (27)–(29) in partial derivatives with the initial conditions (30). As is

known, such a problem has no solution algorithm and needs an individual approach in every special case and it is mathematically hard. In this situation one can consider various limiting cases, which simplifies the full system, so that the problem can be solved completely.

In this section we consider the case where all the desired functions depend on the variables z and t . The solution of this problem gives the evolution of a phonon pulse in the z direction. Clearly this approximation is valid for sufficiently wide pulses in the xy plane where edge effects can be neglected.

In this case, from the initial conditions (30) and the symmetry of the problem, it follows that

$$s_x(z, t) = 0 \quad \text{and} \quad s_y(z, t) = 0 \quad (31)$$

and the system of Eqs. (27)–(29) results in one equation for function $T(z, t)$, which can be rewritten as follows

$$\frac{\partial \rho}{\partial t} + c_\rho \frac{\partial \rho}{\partial z} = 0, \quad (32)$$

where the function

$$\rho = T^4 \quad (33)$$

can be called density, as according to Eq. (17) it determines the density of the phonon energy as a function of time and coordinate,

$$c_\rho = c \left(1 - \frac{\zeta_p}{2} + \varphi_\rho \right) \quad (34)$$

and

$$\varphi_\rho = \frac{1}{4} \frac{d}{dT} \frac{\chi'}{T^2}. \quad (35)$$

The Riemann solution of Eq. (32) with initial condition (30) is the function

$$\rho(z, t) = \rho_0(z - c_\rho t), \quad (36)$$

where the function

$$\rho_0(z - c_\rho t) = T_0^4(z - c_\rho t) \quad (37)$$

is determined by the initial distribution

$$T(z, t=0) = T_0(z). \quad (38)$$

Solution (36) indirectly determines the phonon energy density in various points of the pulse at any moment of time. According to Eq. (36), each value of the density ρ of the pulse moves in space with its own constant velocity c_ρ . In this sense solution (36) is a running wave and is often called a simple wave (see, for example, Ref. 25). Solution (36) describes the result of the summation of two motions: the motion of the phonon pulse in space with velocity $c(1 - \zeta_p/2)$ and the relative motion of different values of ρ with velocity $c\varphi_\rho$.

An explicit expression for the function $\varphi_\rho = \varphi_\rho(\rho = T^4)$ is derived from relations (22) and (35) and looks as follows:

$$\varphi_\rho = \frac{\gamma_d}{3! \zeta(4)} \left(\frac{5!9}{2} \zeta(6) \frac{T^2}{\varepsilon_c^2} - 7!10 \zeta(8) \frac{T^4}{\varepsilon_c^4} \right) = 0.09T^2 - 0.08T^4. \quad (39)$$

According to Eq. (39), the function $\varphi_\rho(T)$ monotonically decreases on both sides from its maximum value, which is equal to 0.025 and occurs at $T=0.75$ K. At temperatures $T=0$ and $T=1.06$ K the function φ_ρ becomes equal to zero. At $T>0.75$ K, φ_ρ decreases and according to Eq. (34) the velocity of motion decreases when the density increases. This result is opposite to the standard situation in hydrodynamics, which takes place in our problem at $T<0.75$ K. The small numerical values of the function $\varphi_\rho \ll 1$ show that the velocity of relative motion, due to different values of T in the pulse, has a relatively small value.

Solution (36) is valid while the function $\rho(z,t)$, given by relations (34) and (36), remains a single-valued function of z . The multiple-valued solution, which appears because different values of density ρ move with different velocities $c_\rho = c_\rho(\rho)$, has no physical sense and results in the creation of a breaking wave (see, for example, Ref. 25). In the region of the multiple-valued solution, the coordinate of the wave-break can be found from the conservation law, according to which at any moment of time

$$\int_{-\infty}^{+\infty} \rho(z,t) dz = \text{const}. \quad (40)$$

At the break, which appears at the point z_{br} , relation (40) becomes

$$\int_{-\infty}^{z_{br}-0} \rho dz + \int_{z_{br}+0}^{+\infty} \rho dz = \text{const}. \quad (41)$$

Taking the derivative of Eq. (41) with respect to time we find the velocity of the break

$$\frac{dz_{br}}{dt} = \frac{\Phi[\rho(z_{br}+0)] - \Phi[\rho(z_{br}-0)]}{\rho(z_{br}+0) - \rho(z_{br}-0)}, \quad (42)$$

where $\Phi(\rho)$ is the indefinite integral of the function $c_\rho = c_\rho(\rho)$, defined in Eq. (34).

From relation (41) it follows that the line of the break in the multiple-valued region divides the area bounded by the multiple-valued line $\rho(z)$ and the line of the break, into two equal parts.

These results enable us to explain the deformation of any initial distribution $T_0(z)$. According to solution (36) and relation (42) the initial rectangular pulse with length $2L_z$ and height T_0 , which is described by the initial distribution

$$T_0(z) = T_0 \eta(L_z - |z|), \quad (43)$$

moves as a whole not changing its form with velocity, which is equal to c within the uncertainties of the experiments.^{1-3,10} This result follows from the instantaneous three-phonon relaxation and accords with experiment. It should be noted that for a pulse of weakly interacting phonons the result is quite different, Ref. 26: an initial rectangular pulse of phonons will become rounded. There are two reasons for this: first, be-

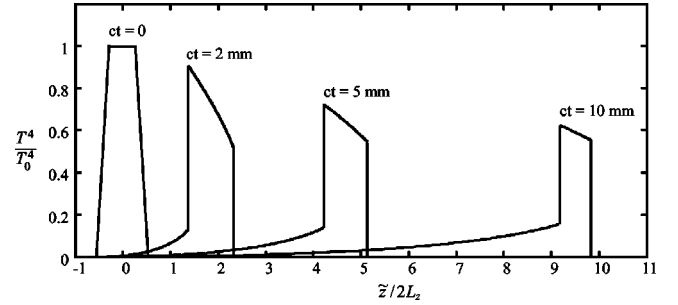


FIG. 1. The evolution of the initial density in the frame of coordinate $\tilde{z} = z - c(1 - \zeta_p/2)t$ that moves relative to the laboratory frame with velocity $c(1 - \zeta_p/2)$. The numerical values $c = 238 \text{ ms}^{-1}$, $\zeta_p = 2 \times 10^{-2}$, $T_0 = 1 \text{ K}$, and $L_z = 0.012 \text{ mm}$ are typical experimental values.

cause phonons in the pulse have different directions, and second, because phonons with different momenta have different group velocities. In spite of the small values of function $\Psi \ll 1$, the group velocities $\partial\varepsilon/\partial p$ for l -phonons with different momenta may differ from one another by $\sim 10 \text{ ms}^{-1}$.

In experiments^{1-3,10} the initial pulse $T_0(z)$ is not exactly rectangular, Eq. (43), because of the time δt_{eq} to reach equilibrium. In experiments $\delta t_{eq} \approx 20 \text{ ns}$ is usually less than the pulse duration t_p . Figure 1 shows an example of a modeled phonon pulse with $t_p = 10^{-7} \text{ s}$ and $\delta t_{eq} = t_p/4$. Comparing the pulses at $ct=0$ and at $ct=10 \text{ mm}$, we see that the pulse is significantly deformed after propagating 10 mm, which is a typical distance for experiments.^{1-3,10} As yet this phenomenon has not been seen but it should be possible in the future to design experiments to measure such changes in the pulse shape. However, it will be shown²⁶ that the pulse presented in Fig. 1, formed by weakly interacting phonons is deformed even more strongly and so should be more easily detected.

It was first suggested in the Ref. 1 that the preservation of the rectangular pulse shape, by the bulk of the pulse during propagation, could be explained by three-phonon interactions. The calculations presented in this section confirm this proposal.

VI. INITIAL EVOLUTION OF THE PULSE IN THE PLANE PERPENDICULAR TO THE DIRECTION OF ITS MOTION

We now consider the case when the required functions, including Eqs. (27)–(29), depend only on the coordinate x and time t . The solution of this problem allows us to study the evolution of a phonon pulse along the x direction, which is perpendicular to the direction of propagation. This approximation is valid for sufficiently large pulses in the z and y directions, where the dependences in these directions can be neglected.

In this case the initial conditions (30) and symmetry of the problem give

$$s_y(x,t) = 0. \quad (44)$$

Equation (29) becomes an identity, and Eqs. (27) and (28) give one-dimensional equations

$$\frac{\partial \rho}{\partial t} + \frac{\partial \rho v}{\partial x} = 0, \quad (45)$$

$$\rho \left\{ \frac{\partial v}{\partial t} + v \frac{\partial v}{\partial x} \right\} = - \frac{\partial P}{\partial x}, \quad (46)$$

where, in accordance with Eq. (33)

$$\rho = T^4 \quad (47)$$

is the density,

$$v = c s_x \quad (48)$$

is a velocity of motion along the axis x ,

$$P = c_\theta^2 \rho \quad (49)$$

is the analog of pressure, and

$$c_\theta = c \sqrt{\zeta_p/2} \quad (50)$$

is the analog of sound velocity which is determined by the angle θ_{3PP} of the cone, in which the phonons are in equilibrium.

The system of Eqs. (45) and (46) should be completed with the initial conditions, which can be written in the following form:

$$\rho(x, t=0) = \rho_0 \eta(L_x - |x|) \quad \text{and} \quad v(x, t=0) = 0. \quad (51)$$

Relation (51) describes a rectangular pulse at $t=0$ with length $2L_x$ and height $\rho_0 = \text{const}$. We should note, that according to the initial conditions (51) and the symmetry of the problem

$$v(x=0, t) = 0. \quad (52)$$

Equations (45) and (46) together with conditions (51) and (52) describe the expansion of a layer of gas into a vacuum. Such an expansion results in the formation of two waves of rarefaction (see, for example, Ref. 27), which during the time interval

$$0 \leq t \leq L_x/c_\theta \quad (53)$$

will propagate in the unperturbed gas, symmetrically to the left ($x < 0$) and right ($x > 0$) (see Fig. 2).

Using dimensional analysis this motion can be described by automodel solutions (see, for example, Ref. 25), in which the functions do not depend on the two variables x and t , but only on one variable $x_t = x_t(x, t)$. In our case

$$x_t = \frac{L_x - |x|}{t}. \quad (54)$$

The dependence of $\rho(x_t)$ and $v(x_t)$ on only one variable allows us to transform the system of two equations, Eqs. (45) and (46), in partial derivatives, into a system of two equations in full derivatives, which has a known algorithm for obtaining the solution.

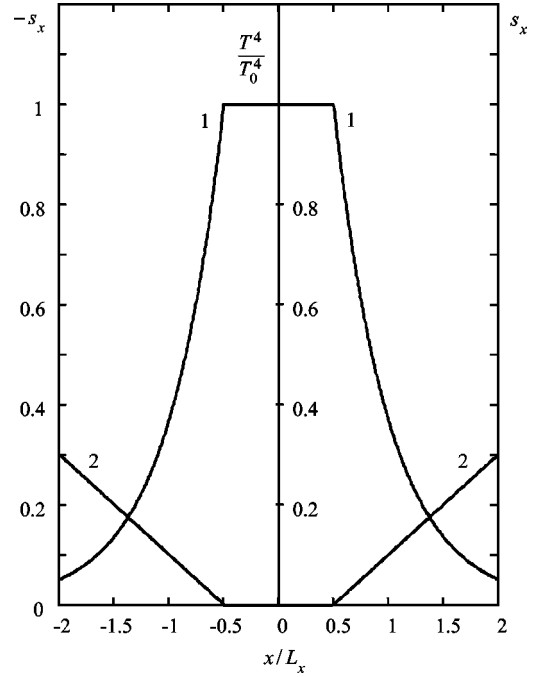


FIG. 2. The dependence of the relative density $\rho/\rho_0 = T^4/T_0^4$ (curve 1) and relative velocity $v/c = s_x$ (curve 2) on the relative coordinate x/L_x at the time moment $t_1 = L_x/2c_\theta$, when the pulse has gone a distance along the axis z equal to $L_{tr} = ct_1 = 2.5$ mm, using typical experimental values $L_x = 0.5$ mm, $c = 238$ ms $^{-1}$, and $\zeta_p = 2 \times 10^{-2}$.

As a result we obtain for the density

$$\rho = T^4 = \begin{cases} \rho_0 & \text{when } 0 \leq |x| \leq L_x - c_\theta t \\ \rho_0 \exp[(L_x - |x| - c_\theta t)/c_\theta t] & \text{when } |x| \geq L_x - c_\theta t, \end{cases} \quad (55)$$

and for the velocity

$$v = c s_x = \begin{cases} 0 & \text{when } 0 \leq |x| \leq L_x - c_\theta t \\ \text{sgn}(x)(|x| - L_x + c_\theta t)/t & \text{when } |x| \geq L_x - c_\theta t. \end{cases} \quad (56)$$

Figure 2 shows the plots of these functions (55) and (56) at the moment $t_1 = L_x/2c_\theta$, when the pulse has gone the distance along the axis z equal to $L_{tr} = ct_1 = 2.5$ mm, calculated with typical experimental data.^{1-3,10} Figure 2 shows that at sufficiently long values of $|x|/L_x$ the value $|s_x|$ is not a very good small parameter. However, according to Fig. 2 and solution (55), at such large values of $|x|/L_x$, the relative density is exponentially small. This satisfies all the derivations made with a quadratic approximation with respect to the small parameter s_x .

Discussion of the results obtained in this section with experimental data will be made in Sec. IX.

VII. LATER EVOLUTION OF PHONON PULSES IN THE PLANE PERPENDICULAR TO THE DIRECTION OF MOTION

Solution (55) and (56) are only valid at all values of x during time interval determined by the inequalities (53). At the time

$$t_r = L_x / c_\theta, \quad (57)$$

the rarefaction wave reaches the point with $x=0$. After that time two reflected waves appear, one each on the left and right. From now on we will consider only the region with positive values $x>0$ since, by symmetry, the solution for $x<0$ is the same as for $x>0$.

The solution that includes the reflected wave $\rho = \rho_r(x, t)$ and $v = v_r(x, t)$ at moments $t > t_r$ will apply in the region

$$0 \leq x \leq x_r, \quad (58)$$

where for times sufficiently close to t_r , we have, from general considerations,

$$x_r = c_\theta(t - t_r) \text{ at } t - t_r \ll t_r. \quad (59)$$

The expression for x_r at arbitrary $t > t_r$ will be derived below during the solution of the problem.

In the region $x \geq x_r$ at time $t > t_r$ the solution for $\rho = \rho(x, t)$ and $v = v(x, t)$ is determined by relations (55) and (56). At the point $x = x_r$ the solution that includes the reflected waves should be joined to solution (55) and (56) for the rarefaction wave to make the function continuous. The derivatives are discontinuous (see Fig. 3). That is why the point x_r is "called a point of weak break." Result (59) expresses the known fact that a weak break moves through the stationary gas at the sound velocity.

As is known the solution that includes the reflected wave is not an automodel one. So, the search for the solution in region (58) is a hard mathematical problem which needs the derivation of a general solution of the system (45) and (46). This is a classical problem of mathematical physics, which has been discussed many times in the scientific literature, (see, for example, Refs. 25,27,28), where it was noted that in the one-dimensional case there exists an exact analytical solution. An analytical expression for the solution of Eqs. (45) and (46) with initial conditions (51) is only presented in Ref. 29 as far as we know. However a numerical analysis of the solution proposed in Ref. 29 has shown that this solution violates the integral conservation law, which follows from Eq. (45). Unfortunately, in Ref. 29 the derivation of this result was not presented, but only described. So we cannot find the reason of this violation.

In this situation we must solve this problem ourselves. Moreover, we use another method of solving which we consider to be more useful. The general solution obtained in this paper, unlike the solution of Ref. 29, includes only single integrals and, therefore, has a simpler analytical form. Our solution satisfies the integral conservation law.

The general solutions of equations (45) and (46) are also applicable in other physical systems. Our derivation is given in the Appendix. To obtain the general solutions of expres-

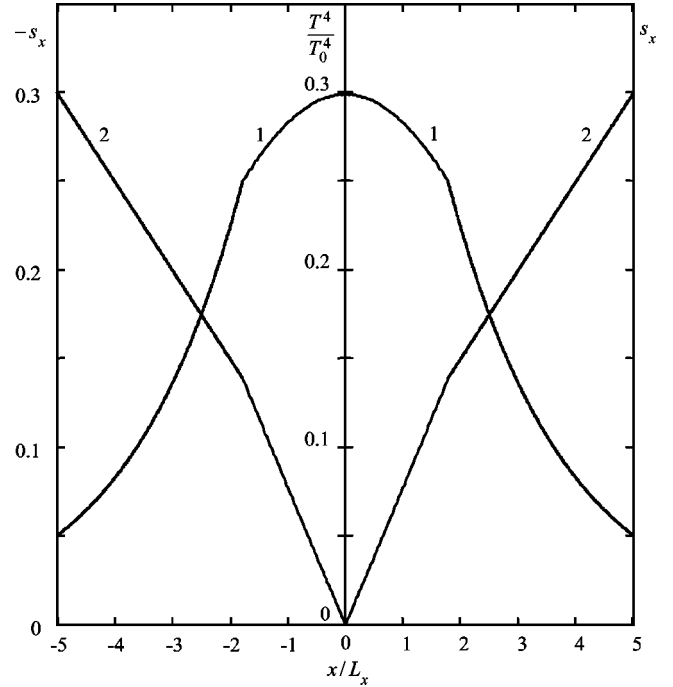


FIG. 3. The dependence of the relative density $\rho/\rho_0 = T^4/T_0^4$ (curve 1) and relative velocity $v/c = s_x$ (curve 2) on the relative length x/L_x at the time moment $t_2 = 2L_x/c_\theta$, when the pulse has gone the distance along the axis z equal to $L_{rr} = ct_2 = 10$ mm, using typical experimental values $L_x = 0.5$ mm, $c = 238$ ms $^{-1}$, and $\zeta_p = 2 \times 10^{-2}$.

sions (45) and (46), which describe the reflected wave, it is useful to introduce new variables α and β , which are connected to the old variables x and t by relations (see the Appendix)

$$t = \frac{1}{4} \frac{L_x}{c_\theta} e^{-\alpha-\beta} \left(\frac{\partial F}{\partial \alpha} + \frac{\partial F}{\partial \beta} - 2F \right), \quad (60)$$

$$x = \frac{L_x}{2} e^{-\alpha-\beta} \left[\left(\alpha - \beta - \frac{1}{2} \right) \frac{\partial F}{\partial \alpha} + \left(\alpha - \beta + \frac{1}{2} \right) \frac{\partial F}{\partial \beta} - 2(\alpha - \beta)F \right], \quad (61)$$

where the function $F(\alpha, \beta)$ satisfies equation (A11) of hyperbolic type with constant coefficients. The general solution of this equation includes two arbitrary functions, which are determined from equality (52) and the condition of joining the general solution to solutions (55) and (56) at the point of the weak break x_r . As the result, we get [see Eqs. (A12), (A15), (A18)]

$$F(\alpha, \beta) = 2 \int_0^\alpha (\kappa - 1) e^{\kappa} I_0(2\sqrt{\beta(\alpha - \kappa)}) d\kappa + 2 \int_0^\beta (\kappa - 1) e^{\kappa} I_0(2\sqrt{\alpha(\beta - \kappa)}) d\kappa - 4I_0(2\sqrt{\alpha\beta}), \quad (62)$$

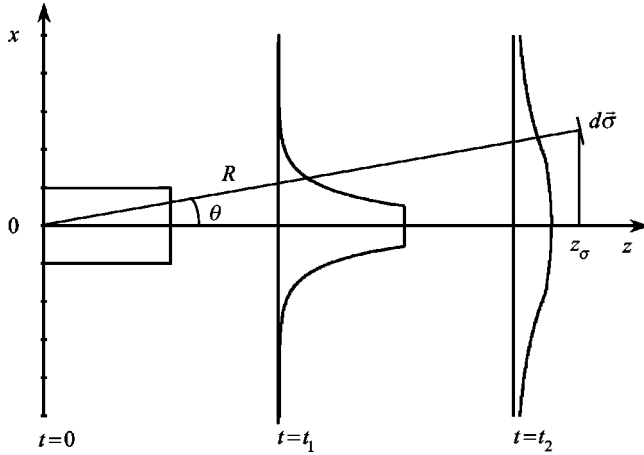


FIG. 4. The evolution of the l -phonon pulse during its travel to the surface element $d\sigma$. The dependence of the relative density in the pulse on coordinate x at time $t=t_1$, curve 1 in Fig. 2, and at time $t=t_2$, curve 1 in Fig. 3.

where I_0 is the modified Bessel function of zeroth order. The solution for the desired functions v and ρ as functions of the new variables α and β can be written as follows:

$$\frac{v}{c} = s_x = \sqrt{2\zeta_p}(\alpha - \beta) \quad \text{and} \quad \frac{\rho}{\rho_0} = \frac{T^4}{T_0^4} = e^{2(\alpha + \beta)}. \quad (63)$$

At $x=0$ Eqs. (60)–(63) give

$$v=0 \quad \text{and} \quad \frac{c\theta t}{L_x} = \frac{T_0^2}{T^2} I_0\left(2 \ln \frac{T_0}{T}\right). \quad (64)$$

The time dependence of the coordinate of the weak break looks like

$$x_r = L_x + \left[2 \ln\left(\frac{c\theta t}{L_x}\right) - 1 \right] c\theta t \quad \text{at} \quad t \geq L_x/c\theta. \quad (65)$$

Figure 3 shows the plot of solutions (60)–(63) at $|x| \leq x_r$ and solutions (55)–(56) at $|x| > x_r$ at the moment $t_2 = 2L_x/c\theta$, when the pulse has reached the distance $ct_2 = 10$ mm along the z axis. The results obtained in this section will be discussed in Sec. IX.

VIII. ANGULAR DEPENDENCE OF THE ENERGY FLUX

In Refs. 2,10 are the results of measurements of the angular dependence of the phonon beam. The pulse of l -phonons is detected by a bolometer, which is at an angle θ with respect to the heater normal.

In order to compare the theory presented in this paper with experimental data,^{2,10} we calculate the flux of energy through the surface element $d\sigma$, which is at an angle θ with respect to the direction of propagation of the pulse. The situation considered here is shown in Fig. 4, which reflects the experimental arrangement.^{2,10}

The energy flux dE_σ through the surface element $d\sigma$ during time dt is equal to

$$dE_\sigma = \mathbf{Q}_E d\sigma dt = (Q_{Ez} \cos \theta + Q_{Ex} \sin \theta) d\sigma dt. \quad (66)$$

Then we substitute Eq. (24) into Eq. (66) and omit the terms that involve the small parameters $\zeta_p \ll 1$ and $\chi/T^4 \ll 1$. As a result we get

$$\frac{dE_\sigma}{d\sigma dt} = \frac{3! \zeta(4) k_B^4}{(2\pi c)^2 \hbar^3} \zeta_p T^4(x, z, t) [\cos \theta + s_x(x, z, t) \sin \theta] \quad (67)$$

The arguments x and z in expression (67) should be considered equal to coordinates x_σ and z_σ of the element $d\sigma$, for which we have

$$x_\sigma = R \sin \theta, \quad \text{and} \quad z_\sigma = R \cos \theta, \quad (68)$$

where R is the distance from the center of the pulse at the moment $t=0$ to the element $d\sigma$ (see Fig. 4). In this case the right hand side of Eq. (67) differs from zero only during the time interval determined by the inequalities

$$\frac{z_\sigma}{c} - \frac{t_p}{2} \leq t \leq \frac{z_\sigma}{c} + \frac{t_p}{2}. \quad (69)$$

The amplitude of the signal on the element $d\sigma$ is determined by the full energy flux through the surface element $d\sigma$, which can be obtained by integrating expression (67) with respect to time in the limits obtained from inequalities (69)

$$I(R, \theta) = \frac{3! \zeta(4) k_B^4}{(2\pi c)^2 \hbar^3} \zeta_p \int_{z_\sigma/c - t_p/2}^{z_\sigma/c + t_p/2} T^4(x_\sigma, z_\sigma, t) \times [\cos \theta + s_x(x_\sigma, z_\sigma, t) \sin \theta] dt. \quad (70)$$

Taking into account the small values of t_p under the integral in Eq. (70) one can substitute t with z_σ/c , and approximate the dependence on z_σ with the step η function. As the result we obtain

$$\frac{I(R, \theta)}{I(R, \theta=0)} = \frac{T^4(x=R \sin \theta, t=R \cos \theta/c)}{T^4(x=0, t=R/c)} \times [\cos \theta + s_x(x=R \sin \theta, t=R \cos \theta/c) \sin \theta]. \quad (71)$$

Figure 5 shows the dependence of the relative energy flux, Eq. (71), on angle θ , which was obtained from the solution of Eqs. (55), (56), and (60)–(63). The numerical values of the parameters were taken from experiments.^{2,10} The denominator in expression (71) is calculated using the relatively simple expression (64). The result is sensitive to the values of the angle θ_{3pp} (see comments at the end of Sec. III). That is why in Fig. 5 we show three curves: curve 1 for $\theta_{3pp} = 11.4^\circ$ ($\zeta_p = 2 \times 10^{-2}$), curve 2 for $\theta_{3pp} = 9^\circ$, and curve 3 for $\theta_{3pp} = 7^\circ$.

The dashed curve 4, in Fig. 5, refers to the angular dependence of the relative flux (71) calculated with the model of geometric broadening, considered in Refs. 30,9,7 with $\theta_{3pp} = 11.4^\circ$. In this model it is supposed that the pulse of

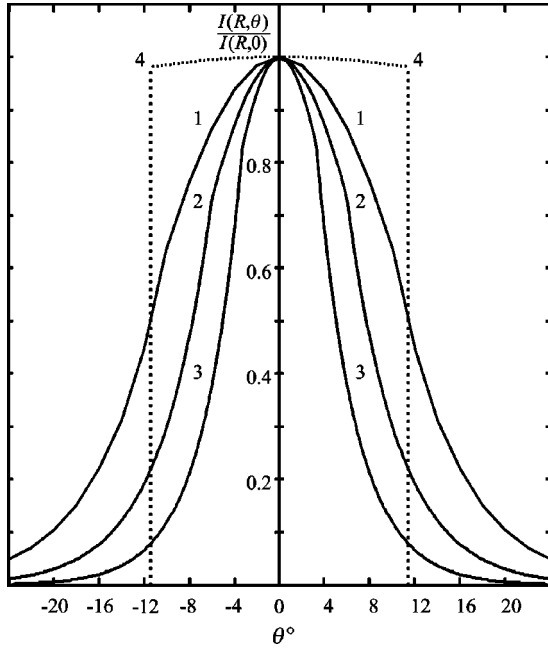


FIG. 5. The dependence of the relative energy flux and signal amplitude on the angle θ between pulse cross-section and detector surface. (a). The angular dependence of the relative energy flux, calculated by equations Eqs. (55), (60)–(64), (71) (solid line) using numerical values $L_x=0.5$ mm, $R=17$ mm, $c=238$ ms $^{-1}$, which are typical experimental values.¹⁰ Lines 1, 2, and 3 are for $\theta_{3PP}=11.4^\circ$ ($\zeta_p=2\times 10^{-2}$), 9° and 7° , respectively. (b). The angular dependence of the relative energy, calculated by Eq. (71) using the model of geometrical broadening in a cone of angle $\theta_{3PP}=11.4^\circ$ (dashed curve 4).

l -phonons, with fixed value of $2L_z$, uniformly occupies all the volume inside the cone with the angle θ_{3PP} , during its motion along the axis of the cone. It was assumed that temperature becomes instantaneously the same at all points in the pulse, which is bounded by two planes separated by $2L_z$ and the surface of the cone with the angle θ_{3PP} with respect to the z axis.

In the model of geometric broadening the second term in the braces in Eq. (71) is equal to zero and the angular dependence at $\theta < \theta_{3PP}$ is given by the function $\cos \theta$.

We see that the curves 1, 2, and 3 in Fig. 5 have a similar form to the experimental curves in Fig. 4 in Ref. 10, whereas the dashed curve 4 is essentially different.

IX. DISCUSSION

We only expect the theory presented in this paper to be comparable with experimental results when the pulse length is sufficiently short and the input power sufficiently low so that h -phonon creation can be neglected.

According to results in Ref. 10 at fixed pulse length $t_p=5\cdot 10^{-8}$ s, with increasing power the angular dependence of l -phonon amplitude signal becomes more flat. As the result, an increase in input power causes the shape of the curve to change with an increase in the full width at half maximum. Similar changes in the angular dependence occur with increasing pulse length at fixed power.

This change of the angular dependence of the signal amplitude with increase of power and pulse length originates from the unusual evolution of the l -phonon pulse, which is determined by solutions (55), (56), and (60)–(63). Let us discuss the mechanism of such a change.

An increase in the input power causes a larger initial temperature T_0 of the l -phonon pulse. At sufficiently high temperatures, the evolution of the l -phonon pulse is determined not only by the mechanism described by Eqs. (55), (56), and (60)–(63), but also by h -phonon creation in the pulse of l -phonons,⁴ which is not considered in this paper. However, it is possible to give a qualitative explanation of the change in evolution of l -phonon pulse when h -phonons are created.

Let us suppose that at the moment $t=0$ we have a l -phonon pulse of rectangular form and distribution function (4) with a relatively high value of T_0 such that high-energy phonons can be created very intensively.^{4,5,7} These h -phonons weakly interact with the l -phonon pulse and have group velocity $v_{gr}\leq 189$ m/s, which is lower than the velocity of the l -phonon pulse. So, once created, the h -phonons will leave the l -phonon pulse through its back wall, and then move relatively slowly to the detector.

While the dependence of $T(x,y)$, throughout the cross section of the l -phonon pulse, is close to a step function, h -phonons are radiated at each point along the back wall of the l -phonon pulse. This results in uniform cooling.

According to solution (55) the evolution of the outer regions of the l -phonon pulse shows the temperature exponentially decreasing from its maximum value to zero. The maximum value of temperature occurs in the region near the axis of the pulse where it forms a “hot spot” (typically 1 K) (see Figs. 2 and 4). The creation of h -phonons only takes place in this central region and in the nearby parts of the outer regions that are hot enough. This process causes this spot to cool, but the outer regions of the pulse, which have a relatively low temperature, do not create h -phonons and so do not cool significantly.

According to the result of calculations in Refs. 4,5,7 the creation of h -phonons is intensive only in the regions with the temperature $T>0.8$ K. This process becomes very slow as soon as temperature decreases to the value ~ 0.7 K. That is why the outer regions with $T<0.7$ K will remain at the same temperature, unlike the central hot region with initially $T\sim 1$ K, which will cool down to $T\sim 0.7$ K by intensively creating h -phonons. As a result, pulses that are initially hotter, cool over a wider area than initially cooler pulses, and so have a temperature distribution that is flat over a larger radius.

However a cool l -phonon pulse, which does not create h -phonons, will have a central hot spot for a typical time t_r , determined by equality (57). During this time the pulse moves a distance

$$L_s = ct_r = \sqrt{\frac{2}{\zeta_p}} L_x = 5 \text{ mm.} \quad (72)$$

During the time $t>t_r$, the pulse temperature, in the center of the pulse, monotonically decreases with the dependence given by Eq. (64), and the temperature at each point of the

pulse decreases. This overall decrease in temperature gives a narrower angular dependence of the signal compared to a hot pulse, in which most of the cooling takes place in the center region due to the creation of h -phonons.

Value (72) can explain the large measured distance over which the l -phonon pulse creates h -phonons.¹

Let us discuss the possible reasons for the width of the flat angular dependence of l -phonon amplitude as a function of the pulse length of the l -phonon pulse, at fixed input power. According to the results of Refs. 5,7 for pulses with the same initial temperature, longer pulses of l -phonons radiate h -phonons for a longer time. As a result, in longer l -phonon pulses the hot spot in the center of the pulse is cooled by creating h -phonons for a longer time than in shorter pulses.

Different temperature distributions in long and short pulses can be caused by their different developments along the z axis with time. In Fig. 1 we see that as the pulse moves along the z axis there is a decrease in the area that has a sufficiently high temperature to create h -phonons. A long pulse will have a constant temperature in the center over a longer distance along the z axis, compared with a short pulse. As a result, the relative change along the z axis for a long pulse will be less than that for a short pulse and the center remains hotter over a larger distance. Hence the cooling of the hot spot of the long pulse, caused by the intensive creation of h -phonons, results in a wider region of constant temperature than for a short pulse.

We should note that the exact solutions (36), (55), (56), (60)–(63), obtained in the framework of the theory presented in this paper, only partially reflect the experimental situation.^{2,10} So, all the qualitative arguments presented in this section need quantitative development. This is only possible with the solutions of a number of hard problems:

(1) In experiments, the problem has nearly cylindrical symmetry as all parameters depend on the radius r , and not the flat problem considered here. It is not hard, using Eqs. (27)–(29) to write the system of equations for the case of axial symmetry. However, so far we have not managed to find analytical solutions for this system. We have made only preliminary investigations, which have shown that solutions (55), (56), (60)–(63) qualitatively describe the case of axial symmetry. So, for example, the velocity of propagation of a rarefying wave is the same as Eq. (50) and, hence, result (72) does not change. However, the solution of the axially symmetric problem is of great interest.

(2) It is necessary to understand how the dependence of temperature on the coordinate z , changes the evolution of the pulse in its crosssection. The answer to this question can only be obtained from the exact solution of the system of Eqs. (27)–(29) which takes into account the term involving the partial derivatives with respect to different Cartesian coordinates. However, this solution causes some difficulties, which are not yet overcome.

(3) It is necessary to consider the evolution of the l -phonon pulse which takes into account the creation of h -phonons. In order to do this, we should add to the system (27)–(29) the equations that describe the process of h -phonon creation, and then try to solve this system.

A separate, hard, and important problem is the creation and the subsequent evolution of the h -phonon pulse. This problem was not even discussed in this paper, though the data presented in Ref. 10 show it is important. The new experimental data Ref. 10, together with earlier experimental data, Refs. 2,22, is evidence of the nontrivial properties of anisotropic phonon systems. Undoubtedly this will stimulate solving the problems mentioned above and we expect to discover new phenomena in this field of quantum liquids physics.

ACKNOWLEDGMENTS

We would like to thank EPSRC for Grants Nos. GR/S24855/01 and GR/N20225 and GFFI of Ukraine for Grant No. 02.07/000372.

APPENDIX

Let us introduce the velocity potential

$$v = \frac{\partial \varphi}{\partial x} \quad (\text{A1})$$

and the new function

$$w = c_\theta^2 \ln \frac{\rho}{\rho_0}. \quad (\text{A2})$$

Then rewrite systems (45) and (46) as follows:

$$\frac{\partial w}{\partial t} + v \frac{\partial w}{\partial x} + c_\theta^2 \frac{\partial v}{\partial x} = 0, \quad (\text{A3})$$

$$\frac{\partial \varphi}{\partial t} + \frac{v^2}{2} + w = 0. \quad (\text{A4})$$

Now we make the godograph transformation (see, for example, Ref. 25), according to which we introduce new independent variables v , w instead of x , t . In accordance with the Legendre transformation we introduce the function $\mu = \mu(v, w)$ by the equality

$$\mu(v, w) = \varphi - xv + t \left(w + \frac{v^2}{2} \right). \quad (\text{A5})$$

In Eq. (A5) values φ , x , and t are supposed to be functions of the new independent variables v and w .

According to the Legendre transformations

$$t = \frac{\partial \mu}{\partial w} \quad \text{and} \quad x = v \frac{\partial \mu}{\partial w} - \frac{\partial \mu}{\partial v}. \quad (\text{A6})$$

The equation for the function μ is obtained by division of Eq. (A3) by the Jacobian

$$\frac{\partial(w, v)}{\partial(x, t)}, \quad (\text{A7})$$

which for the general solution is not equal to zero. Let us note that for the automodel solution the Jacobian (A7) is

equal to zero. That is why the automodel solution often is called the special solution unlike the general solution considered here. As the result from Eq. (A3) taking into account Eq. (A6) we get

$$c_\theta^2 \frac{\partial^2 \mu}{\partial w^2} - \frac{\partial^2 \mu}{\partial v^2} + \frac{\partial \mu}{\partial w} = 0. \quad (\text{A8})$$

Equation (A8) can be simplified, if instead of the variables w and v we introduce the variables α and β by the equalities

$$v = 2c_\theta(\alpha - \beta), \quad w = 2c_\theta^2(\alpha + \beta) \quad (\text{A9})$$

and a new nondimensional function

$$F = \frac{1}{c_\theta L_x} e^{\alpha + \beta} \mu, \quad (\text{A10})$$

for which, starting from Eq. (A8) we get the equation

$$\frac{\partial^2 F}{\partial \alpha \partial \beta} = F. \quad (\text{A11})$$

The general solution of Eq. (A11) can be written as follows:

$$\begin{aligned} F = & \int_0^\alpha G_1(\kappa) I_0(2\sqrt{\beta(\alpha - \kappa)}) d\kappa \\ & + \int_0^\beta G_2(\kappa) I_0(2\sqrt{\alpha(\beta - \kappa)}) d\kappa \\ & + \{G_1(0) + G_2(0)\} I_0(2\sqrt{\alpha\beta}), \end{aligned} \quad (\text{A12})$$

where $G_1(\kappa)$ and $G_2(\kappa)$ are arbitrary functions, and $I_0(\gamma)$ is the modified Bessel function of zeroth order of argument γ .

From relations (A6), (A9), and (A10), we get

$$t = \frac{L_x}{4c_\theta} e^{-\alpha - \beta} \left[\frac{\partial F}{\partial \alpha} + \frac{\partial F}{\partial \beta} - 2F \right], \quad (\text{A13})$$

$$\begin{aligned} x = & \frac{L_x}{2} e^{-\alpha - \beta} \left[\left(\alpha - \beta - \frac{1}{2} \right) \frac{\partial F}{\partial \alpha} \right. \\ & \left. + \left(\alpha - \beta + \frac{1}{2} \right) \frac{\partial F}{\partial \beta} - 2(\alpha - \beta)F \right]. \end{aligned} \quad (\text{A14})$$

Equalities (A9), (A12)–(A14) give the general solution of system (45) and (46).

The arbitrary functions G_1 and G_2 including Eq. (A12) can be found from the boundary conditions of the particular problem. The first boundary condition follows from equality Eq. (52), taking into account Eqs. (A9), (A12), and (A14) gives

$$G_1(\kappa) = G_2(\kappa). \quad (\text{A15})$$

The second boundary condition comes from joining the general solutions (A9), (A12)–(A14) with the automodel solution at the point x_r which is the point of transition from the general solution to automodel one. Comparing the automodel solutions (55) and (56) with Eq. (A9) it is easy to see that these solutions can be joined only on the characteristics $\alpha = 0$.

The solutions are joined by substituting in the automodel solution

$$x = L_x + (v - c_\theta)t \quad (\text{A16})$$

the expression v , t , and x from solutions (A9), (A13) and (A4), taking into account Eq. (A15) at $\alpha = 0$. This joining, taking into account Eq. (A16) gives the following equation

$$\left(\frac{\partial F}{\partial \beta} - F \right) \Big|_{\alpha=0} = 2e^\beta. \quad (\text{A17})$$

Substituting Eq. (A12) into Eq. (A17) and taking into account Eq. (A15) give an integral equation for G_1 , which by differentiation gives a differential equation. The solution of this differential equation looks like

$$G_1(\kappa) = 2(\kappa - 1)e^\kappa. \quad (\text{A18})$$

Relations (A15) and (A18) solve the problem of finding the functions G_1 and G_2 which occur in Eq. (A12), using the boundary conditions.

The coordinate of the break (65) is found by substituting the value of the velocity at the break into Eq. (A16). This value is found by comparing the expressions for the velocity which follow from relations (A9) and (A13) at $\alpha = 0$.

¹M.A.H. Tucker and A.F.G. Wyatt, J. Phys.: Condens. Matter **6**, 2813 (1994).

²M.A.H. Tucker and A.F.G. Wyatt, J. Phys.: Condens. Matter **6**, 2825 (1994).

³M.A.H. Tucker and A.F.G. Wyatt, J. Low Temp. Phys. **113**, 621 (1998).

⁴I.N. Adamenko, K.E. Nemchenko, A.V. Zhukov, M.A.H. Tucker, and A.F.G. Wyatt, Phys. Rev. Lett. **82**, 1482 (1999).

⁵A.F.G. Wyatt, M.A.H. Tucker, I.N. Adamenko, K.E. Nemchenko, and A.V. Zhukov, Phys. Rev. B **62**, 9402 (2000).

⁶M.A.H. Tucker, A.F.G. Wyatt, I.N. Adamenko, K.E. Nemchenko, and A.V. Zhukov, Phys. Rev. B **62**, 3029 (2000).

⁷I.N. Adamenko, K.E. Nemchenko, and A.F.G. Wyatt, Fiz. Nizk. Temp. **28**, 123 (2002) [J. Low Temp. Phys. **28**, 85 (2002)].

⁸I.N. Adamenko, K.E. Nemchenko, and A.F.G. Wyatt, Fiz. Nizk. Temp. **29**, 16 (2003) [J. Low Temp. Phys. **29**, 11 (2003)].

⁹A.F.G. Wyatt, I.N. Adamenko, and K. E Nemchenko, J. Low Temp. Phys. **126**, 609 (2002).

¹⁰R. V. Vovk, C. D. H. Williams, and A. F. G. Wyatt, following paper, Phys. Rev. B. **68**, 134508 (2003).

- ¹¹H.J. Maris and W.E. Massey, Phys. Rev. Lett. **25**, 1220 (1970).
- ¹²J. Jäckle and K.W. Kerr, Phys. Rev. Lett. **27**, 654 (1971).
- ¹³N.G. Mills, R.A. Sherlock, and A.F.G. Wyatt, Phys. Rev. Lett. **32**, 1978 (1974).
- ¹⁴R.C. Dynes and V. Narayanamurti, Phys. Rev. Lett. **33**, 1195 (1974).
- ¹⁵A.F.G. Wyatt, N.A. Lockerbie, and R.A. Sherlock, Phys. Rev. Lett. **33**, 1425 (1974).
- ¹⁶M.A.H. Tucker and A.F.G. Wyatt, J. Phys.: Condens. Matter **4**, 7745 (1992).
- ¹⁷S. Havlin and M. Luban, Phys. Lett. **42A**, 133 (1972).
- ¹⁸M.A.H. Tucker, A.F.G. Wyatt, I.N. Adamenko, A.V. Zhukov, and K.E. Nemchenko, Fiz. Nizk. Temp. **25**, 657 (1999) [J. Low Temp. Phys. **25**, 488 (1999)].
- ¹⁹I.N. Adamenko, K.E. Nemchenko, and A.F.G. Wyatt, J. Low Temp. Phys. **126**, 1471 (2002).
- ²⁰I.N. Adamenko, K.E. Nemchenko, A.V. Zhukov, M.A.H. Tucker, and A.F.G. Wyatt, Physica B **284–288**, 33 (2000).
- ²¹I.M. Khalatnikov, D.M. Chernikova, Zh. Eksp. Teor. Fiz **49**, 1957 (1965) [Sov. Phys. JETP **22**, 1336 (1966)].
- ²²R.A. Sherlock, N.G. Mills, and A.F.G. Wyatt, J. Phys. C **8**, 2575 (1975).
- ²³I.N. Adamenko, M.I. Kaganov, Zh. Eksp. Teor. Phys. **53**, 886 (1967) [Sov. Phys. JETP **26**, 537 (1968)].
- ²⁴V.L. Gurevich, B.D. Laikhtman, Zh. Eksp. Teor. Phys. **70**, 1907 (1976) [Sov. Phys. JETP **43**, 993 (1976)].
- ²⁵L. D. Landau and E. M. Lifshitz, *Hydrodynamics* (Nauka, Moscow, 1988); *Fluid Mechanics* (Pergamon Press, Oxford, 1987).
- ²⁶I.N. Adamenko, K.E. Nemchenko, V.A. Slipko, and A.F.G. Wyatt (unpublished).
- ²⁷K. P. Stanyukovich, *Unsteady Motion of Continuous Media* (Nauka, Moscow, 1971); *Unsteady Motion of Continuous Media* (Pergamon Press, London, 1960).
- ²⁸Ya. B. Zel'dovich and Yu. P. Raizer, *The Physics of Shock Waves and High-Temperature Hydrodynamics* (Nauka, Moscow, 1963) (in Russian).
- ²⁹V.S. Imshennik, Dokl. Akad. Nauk **131**, 1287 (1960) [Sov. Phys. Dokl. **5**, 253 (1960)].
- ³⁰C.D.H. Williams, A.A. Zakharenko, and A.F.G. Wyatt, J. Low Temp. Phys. **126**, 591 (2002).